

# The Metal Grating Design of Plasmonic Hybrid III-V/Si Evanescent Lasers

Min-Hsiang Hsu<sup>1</sup>, Chien-Chung Lin<sup>1\*</sup>, and Hao-Chung Kuo<sup>2</sup>

<sup>1</sup> Institute of Photonic System,

National Chiao Tung University, Tainan 711, Taiwan

<sup>2</sup> Department of Photonics and Institute of Electro-Optical Engineering,

National Chiao Tung University, Hsinchu 30010, Taiwan

\* E-mail address: chienchunglin@faculty.nctu.edu.tw

## Abstract

The plasmonic hybrid III-V/Silicon evanescent lasers employing metal gratings have been theoretically demonstrated. The optimized threshold gain is of the order  $0.6 \mu\text{m}^{-1}$ , comparable to current nanolasers and showing the possibility to be realized.

## 1. Introduction

Since electrically-pumped hybrid III-V/silicon evanescent laser was reported in 2006, such device designs have become popular [1]. Several improvements in hybrid laser cavity designs [2], passive waveguide structure [3], epitaxial materials [4], and bonding process [5] have been demonstrated to achieve better performance than the prototype. Despite the impressive device performance of those demonstrations, the dimensions of the silicon waveguide in above devices still fall behind what the photonic roadmap predicts [6]. If this roadmap needs to be followed and the passive waveguide is shrunk down to hundreds of nanometer scale, below the cut-off dimensions, the waveguide will not be able to support the mode anymore, and leading to design failure [6]. Therefore, we propose a plasmonic hybrid III-V/Si evanescent laser, as shown in the Fig. 1(a), which combines the merits of optical gain of III-V chip and small dimension of plasmonic waveguide, to achieve a feasible Si-based laser design in a nano-scale platform. In this paper, the numerical study of such design will be performed, and general device dimensions and performance will be evaluated through simulations.

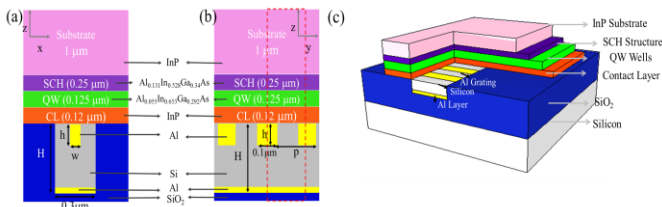


Fig. 1. The schematics of the proposed hybrid III-V/Silicon evanescent lasers.

## 2. Simulation Model

A 3-dimensional (3-D) eigenmode calculation at wavelength  $1.55 \mu\text{m}$  was established by the finite-element method (FEM) using COMSOL differential equation solver. The III-V structure in our proposed device, as shown in Fig. 1(b) and 1(c), consists of  $1\text{-}\mu\text{m}$  InP substrate,  $0.25\text{-}\mu\text{m}$   $\text{Al}_{0.13}\text{In}_{0.528}\text{Ga}_{0.34}\text{As}$  separated confinement heterostructure

(SCH),  $0.125\text{-}\mu\text{m}$   $\text{Al}_{0.055}\text{In}_{0.653}\text{Ga}_{0.292}\text{As}$  quantum well (QW) and  $0.12\text{-}\mu\text{m}$  InP contact layer, respectively. The height of the embedded silicon waveguide,  $H$ , can be treated as one of the variables, and the width of the waveguide is fixed at  $300\text{nm}$ ; the thickness of Al layer located at bottom of the silicon ridge waveguide is  $0.05 \mu\text{m}$ . The dimensions of metal gratings are  $h$  in depth,  $w$  in width and  $0.1 \mu\text{m}$  in length and their periods are  $p$  ( $h$ ,  $w$ , and  $p$  will be used as design variables in the latter contents.).

In order to address the real application and determine the optimization criterion of our proposed design, the threshold gain in a general laser device can be calculated by the formula:

$$g_{\text{th}} = (n_{\text{eff}(r)}/n_{\text{QW}}) [4\pi n_{\text{eff}(i)}/\lambda + \ln(1/R^2)/(2l)]/\Gamma_{\text{QW}} \quad (1)$$

where  $g_{\text{th}}$  is threshold gain,  $n_{\text{eff}(r)}$  and  $n_{\text{eff}(i)}$  is effective index of real part and imaginary part, respectively,  $\lambda$  is free wavelength  $1.55 \mu\text{m}$ ,  $R$  is reflectivity,  $l$  is waveguide length assumed to be  $30 \mu\text{m}$ ,  $\Gamma_{\text{QW}}$  is power confinement in quantum wells and  $n_{\text{QW}}$  is the refractive index equal to  $3.6594$  [7]. Note that we also assume the reflection loss is resulted from dielectric-air Fresnel reflection instead of from mirrors or any other reflectors. Therefore,

$$R = [(n_{\text{eff}} - 1)/(n_{\text{eff}} + 1)]^2 \quad (2)$$

Low threshold gain indicates low loss for the system, but mode distribution in waveguide cavity and III-V gain medium should be considered simultaneously. Owing to multiple device structure parameters needed to be determined, the waveguide height ( $H$ ), grating depth ( $h$ ), width ( $w$ ) and period ( $p$ ) are chosen to be optimized.

## 3. Results & Discussion

First, the embedded ridge height ( $H$ ) and Al grating depth ( $h$ ) are set as variables to test their influences on the optical behaviors, and, in the beginning, grating width ( $w$ ), height ( $h$ ) and period ( $p$ ) are  $0.1$ ,  $0.1$  and  $0.3 \mu\text{m}$ , respectively. When we increase the height of buried silicon waveguide from  $0.3$  to  $0.9 \mu\text{m}$ , transformation in optical field distribution is expected. In the short waveguide height, only surface plasmonic polariton (SPP) mode on the bottom of Al layer is possible (like in  $0.3 \mu\text{m}$  case of Fig. 2(b)). However, if the waveguide ridge is too high, as in Fig. 2(d), multiple SPP modes can be seen in the waveguide. When the design falls in between these two situations, it will be

the best for the lasers device (as in Fig. 2(c)). Therefore, the ridge height is fixed at  $0.6 \mu\text{m}$  to ensure there is only one circular guided mode supported in the waveguide. Then, we simultaneously change the width and height of metal gratings, and calculate their field distributions and threshold gains, as shown in the Fig. 3. In the Fig. 3(a), the device with the metal grating width  $0.3 \mu\text{m}$  exhibits the lowest threshold gain. At the metal grating with width  $0.3 \mu\text{m}$ , the device with  $0.1 \mu\text{m}$  grating depth is suitable for device because not only the device has less threshold gain but also equal energy distribution in QW and waveguide can be established such that the light can transmit in the III-V material and silicon structure simultaneously, as energy distributions shown in the Fig. 3(b).

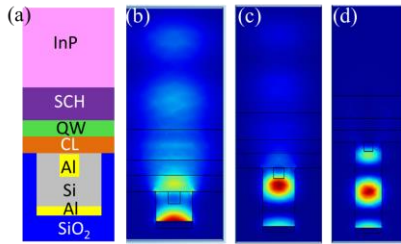


Fig. 2. (a) the corresponding schematic to the simulated energy density distribution results with (b)  $0.3 \mu\text{m}$ -, (c)  $0.6 \mu\text{m}$ -, and (d)  $0.9 \mu\text{m}$ -high waveguide.

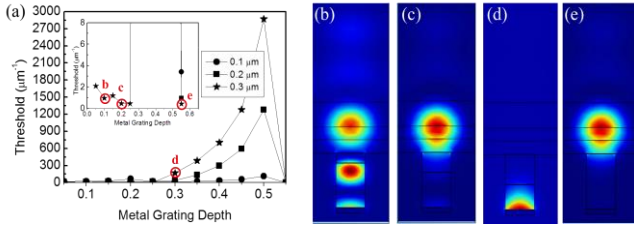


Fig. 3. (a) The calculated threshold gain of the device. The inset just zooms in the range of threshold gain from  $0$  to  $8 \mu\text{m}^{-1}$ . The corresponding energy density distribution with (b)  $0.1 \mu\text{m}$ -, (c)  $0.2 \mu\text{m}$ -, (d)  $0.3 \mu\text{m}$ -, and (e)  $0.55 \mu\text{m}$ -deep gratings, which are labeled in the (a) via red circles.

Finally, the grating period is varied systematically to examine the field distribution and the threshold gain. The power distribution undulates corresponding to the metal grating period, leading the threshold gain to oscillate as well. The threshold gain becomes stable to  $0.5 \mu\text{m}^{-1}$  ( $=5000 \text{cm}^{-1}$ ) when the metal grating separation is large as shown in the Figure 4(a). From the cross-section view of field distribution, the distribution of energy oscillates back and forth between the waveguide and QW regions. When the field is concentrated in the upper QW part, the threshold tends to be the lowest. On the other hand, when field maximized in the silicon waveguide region, the threshold gain increases sharply. The balance between the requirement of light transmission and lasing operation is an important issue for the engineer to decide, and a suitable combination of the two extremes (energy in QW or silicon waveguide) can generate the best working device such that the energy can be transmitted inside the waveguide and replenished by the gain of QW at the same time. In our simulation, we believe

the case of period  $0.73 \mu\text{m}$  (Fig. 4(f)) should be most suitable for the generic design because of its balanced field distribution between QW and silicon plasmonic waveguide, corresponding to the threshold gain  $0.62 \mu\text{m}^{-1}$ .

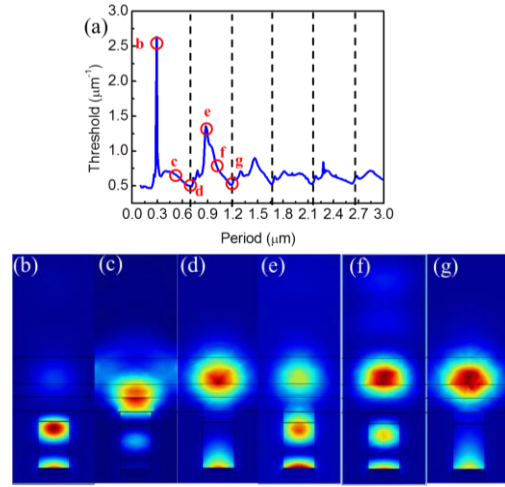


Fig. 4. (a) The calculated threshold gain of the device. The corresponding energy density distribution with the grating period at (b)  $0.29 \mu\text{m}$ , (c)  $0.5 \mu\text{m}$ , (d)  $0.73 \mu\text{m}$ , (e)  $0.87 \mu\text{m}$ , (f)  $0.93 \mu\text{m}$  and (g)  $1.21 \mu\text{m}$ , which are labeled in the (a) via red circles.

#### 4. Conclusions

We propose a method to fabricate nano-scaled hybrid III-V/Silicon laser device by incorporating the plasmonic effect from the embedded metal grating. The calculated gain threshold  $0.62 \mu\text{m}^{-1}$  of the optimized device shows great potential to realize this design in practice.

#### Acknowledgements

This work is sponsored by the financial supports from National Science Council of Taiwan through the contract numbers of NSC 101-2221-E-009-046-MY3.

#### References

- [1] A. W. Fang, H. Park, O. Cohen, R. Jones, M. J. Paniccia, and J. E. Bowers, *Opt. Express* **14**, (2006) 9203.
- [2] A. J. Zilkie, P. Seddighian, B. J. Bijlani, W. Qian, D. C. Lee, S. Fatholouloumi, J. Fong, R. Shafiiha, D. Feng, B. J. Luff, X. Zheng, J. E. Cunningham, A. V. Krishnamoorthy, and M. Asghari, *Opt. Express* **20**, (2012) 23456
- [3] A. W. Fang, E. Lively, Y. H. Kuo, D. Liang, and J. E. Bowers, *Opt. Express* **16**, (2008) 4413.
- [4] X. Sun, A. Zadok, M. J. Shearn, K. A. Diest, A. Ghaf-fari, H. A. Atwater, A. Scherer, and A. Yariv, *Opt. Lett.* **34**, (2009) 1345.
- [5] D. Liang, G. Roelkens, R. Baets, and J. E. Bowers, *Materials* **3**, (2010) 1782.
- [6] W. L. Barnes, A. Dereux, and T. W. Ebbesen, *Nature* **424** (2003) 824.
- [7] H. Dejun, in *Proceedings of IEEE Lasers and Electro-Optics Society Annual Meeting*, **2**, (1994) 349.